# Acidity of zeolite Y—Probed by adsorption of 1-naphthylamine and studied by laser-induced fluorescence spectroscopy

Ali A. El-Rayyes, H.P. Perzanowski, Uwe K.A. Klein, and Sami A.I. Barri *

*Chemistry Department, King Fahd University of Petroleum and Minerals, Dhahran 31261, Saudi Arabia*

Received 5 June 2001; accepted 3 October 2001

Proton transfer reactions between zeolite Y surface and 1-naphthylamine (NA) in the ground and excited states have been studied by laser-induced picosecond spectroscopy. The acidic form of zeolite Y readily protonates NA in the ground state. At low acid strength of the zeolite the excited state of the protonated NA transfers back the proton to the zeolite surface as indicated by the fluorescence spectra. At high acid strength of the zeolite the fluorescence comes from the protonated form of NA and from an adduct "X" previously found in highly concentrated $HClO_4$ solutions. The concentrations of the protonated NA and X increase with the reduction in the unit cell size. The presence of these species is discussed in terms of the next nearest neighbor "NNN" theory of zeolite Y acidity and the role of the non-framework aluminum. The acidity of the zeolite is estimated, based on the fluorescence lifetimes of X, to vary from 3.7 to 17 M $HClO_4$ depending on the unit cell size. Low loading levels of NA in the zeolite pores are best in studying the proton transfer reaction and for the estimation of the surface acidity of zeolite Y.

**KEY WORDS:** acidity; laser; 1-naphthylamine; spectroscopy; zeolite Y

## 1. Introduction

Solid acids, especially zeolites, are widely used as catalysts in industry [1–9]. The catalytic performance strongly depends on the concentration and strength of the acid site on the surface of the solids. Both of these factors can be modified on the surface of zeolite catalysts with some degree of control in the synthesis stage by varying the Si/Al ratio or in a post synthesis treatment such as steaming or chemical dealumination [7,10,11]. The framework Si/Al ratio has a fundamental impact on the stability of zeolite Y and its acidity. In fluid catalytic cracking ultrastable zeolite Y (USY) is used with great success because of its high acidity and hydrothermal stability. Determination of the surface acidity is of importance to the understanding of the reactions occurring on the internal surface of the micropores of the catalysts. It is increasingly understood that at low Si/Al ratio the average acid strength increases with dealumination due to the superior strength of the isolated site and in siliceous zeolite the acid strength depends only on the crystallographic site of the aluminum. Zeolite Y is one of the most studied zeolites because of its important application in catalysis. Complete ion exchange of the sodium cations with ammonium renders the zeolite hydrothermally unstable if the concentration of the aluminum in its framework is high enough. The term "ultrastable faujasite" was coined by McDaniel and Maher [7], when they described the calcination of the ammonium form of the zeolite in a regime that led to the incipient steaming of the zeolite. Such treatment also led to a reduction in the unit cell size as a large proportion of the framework aluminum was replaced by silicon. Kerr [8] proposed that deep bed calcination results in the self-steaming of the zeolite and leads to the ultrastable form. It has been established since that controlled steaming of the zeolite also gives a stable zeolite. In addition to the stabilization of the proton form of the zeolite, removal of aluminum from the framework leads to an overall increase in the acid strength per site as the proportion of the isolated sites with zero next nearest neighbor (0-NNN) sites is increased [12].

Zeolite acidity can be evaluated by a number of techniques such as the temperature-programmed desorption of bases, calorimetric methods, FTIR, or the use of test catalytic reactions [4]. These techniques give qualitative or semi-quantitative evaluation of acidity but can be used to rank a closely related set of zeolite catalysts. In the 1970's, Hammett indicators were used to establish an acidity scale for zeolites based on the $pK_a$ values [5]. The limitations of this method were the use of bulky indicator molecules that interacted with the surface of the catalyst and gave unrepresentative readings. More recently, interaction of probe molecules with acidic sites were investigated photochemically *via* their fluorescence properties [13–28]. Some of these studies have utilized laser-induced fluorescence of adsorbed molecules to study the nature of the interaction with the substrate surface. We report, in this paper, on the proton transfer reaction between the zeolite Y surface and 1-naphthylamine (NA) in the ground and excited state by laser-induced picosecond spectroscopy. We also propose an acidity scale for this particular system. This study makes use of our published work on the fluorescence properties of NA and its protonated form in highly concentrated aqueous perchloric acid [32]. Transparent films [29–31] of the zeolite in poly-

* To whom correspondence should be addressed. E-mail: sabarri@kfupm.edu.sa

1011-372X/02/0300-0161/0 © 2002 Plenum Publishing Corporation

dimethylsiloxane (PDMS) are used, as results obtained using zeolite powder are prone to difficulties due to scattered light, in particular in the UV region.

## 2. Experimental

### *2.1. Materials*

Zeolite Y was Linde Zeolite LZ 52Y, which is the sodium form of zeolite Y, here denoted as NaY. Samples with varying degrees of the proton forms were prepared by ion exchanging the parent zeolite NaY with ammonium nitrate solution. A sample containing 34% $NH_4^+$ and 66% $Na^+$ was prepared by stirring NaY in 0.25 M solution of ammonium nitrate for 30 min at room temperature (24 °C). The liquid to zeolite ratio was 4 : 1 by weight. The zeolite was filtered, washed and dried at 110 °C for 6 h. It was then calcined at 450 °C for 24 h raising the temperature from room temperature at the rate of 1°/min. This sample was denoted as HY-34, as 34% of the exchange sites were in the H-form. Similarly the samples HY-60, HY-73, HY-83, and HY-96 were prepared by successive ion exchange with ammonium nitrate solution followed by drying and calcination as above.

The ultrastable zeolite Y was prepared following the McDaniel and Maher [7] procedure but the calcination steps were carried out in a tubular reactor in the presence of flowing steam and air. The air flow rate measured at room temperature, for a 5 g quantity of zeolite, was 80 ml/min whereas the water was fed at 20 ml of liquid per hour.

X-ray powder diffraction measurements were carried out using a Siemens D5005 instrument. Each sample was gently ground in an agar pestle and mortar. The fine powder was packed into a sample holder having a diameter of ∼25 mm and depth of ∼3 mm. The surface of the packed sample was smoothened with a piece of flat glass. The diffraction pattern was recorded from 0.4° to 50° 2-Theta. A step scan of 0.010° 2-Theta was used, counting at every step for 3 s. The divergence and anti-scattering slits were varied by setting these at v20. This setting kept the irradiated sample area constant at approximately 20 mm × 12 mm. The voltage and current of the generator were set at 40 kV and 30 mA, respectively.

Adsorption measurements were carried out on a Hiden Analytical IGA system (gravimerical measurement). Aliquots of the sample being measured (∼100 mg) were loaded and evacuated at *ca.* $10^{-7}$ mbar. The temperature was then raised to 400 °C at the rate of 5 °C/min for the furnace temperature. However, because of the high vacuum, the sample temperature only rose to 340 °C. After 3 h at the final temperature and high vacuum, the sample was cooled to ambient and then to 15 °C using a circulating chilled liquid system. When the conditions equilibrated, small pulses of benzene vapor were introduced periodically *via* a gas admittance valve which was electronically controlled to obtain adsorption steps of approximately 2 wt%. This gave rise to an isotherm comprising about 50 equilibrium points in each direction. At each period of pressure, the equilibrium was attained before another pulse of the adsorbate was introduced. The sample weight was recorded on a highly accurate microbalance and the pressure of the adsorbate was measured using a set of pressure transducers, each calibrated to measure the pressure at a specific range. The conditions (pressure and temperature), operation control, and data processing were handled by a manufacturer designed software.

Magic angle spinning NMR (MAS-NMR) of $^{29}Si$ and $^{27}Al$ spectra of spectral width of 20 000 Hz were recorded at 11.74 T on a Joel JNM-LA 500 spectrometer. The frequencies for $^{29}Si$ and $^{27}Al$ were 99.25 and 130.28 MHz, respectively. A 90° pulse width, which is a pulse length of 6 $\mu$s, with a repetition time of 15 s was used. The number of scans was 500 and the spin rate of the sample tube was 4.0 kHz. The number of scans for the $^{27}Al$ spectra of the USY sample was 1500. Chemical shifts for the $^{29}Si$ were reported relative to poly(dimethysilane), while aluminum sulfate hydrate was used as a reference for the $^{27}Al$ chemical shifts.

1-naphthylamine was supplied by the Fluka company and was used after recrystallisation from petroleum ether followed by sublimation. Solvents such as *n*-hexane (spectral grade) are used after drying over molecular sieves 5A. Polydimethylsiloxane (PDMS) was provided by General Electric silicones.

### *2.2. Preparations of solid-organic probe complex*

Aliquots of zeolite Y were calcined at 500 °C overnight and cooled in a desiccator under vacuum. The dried solid was transferred into a solution of the 1-naphthylamine in *n*-hexane and stirred for about 6 h and kept overnight to reach equilibrium. The complex was then collected by filtration and washed three times with the solvent to remove the externally adsorbed NA molecules and then dried on a vacuum line at $10^{-3}$–$10^{-4}$ Torr. The percent loading of the fluorophore on the molecular sieves is calculated by comparing the UV spectra of the original solution to that of the filtrate. The NA/*n*-hexane concentrations used for various loadings were: $1.83 \times 10^{-2}$, $9.75 \times 10^{-3}$, $1.10 \times 10^{-3}$, and $1.30 \times 10^{-4}$ M.

The PDMS membrane of the zeolite loaded with NA was prepared as follows: 30–70 mg of the dried zeolite loaded with the NA molecules was transferred into a vial containing 1 g of *n*-hexane. The mixture was sonicated for a period of 1 h to break the zeolite aggregates. Then 1 g of RTV 615 A was added and the mixture was sonicated again for a period of 6 h. Finally, 100 mg of RTV 615 B was added and the mixture was further sonicated for 20 min. The mixture was cast onto a glass plate and heated in an oven at 60 °C overnight. The membrane was removed from the glass plate and further dried at 60 °C for a few hours.

UV-Vis absorption measurements of the solutions used were recorded using a λ-5 (Perkin–Elmer) spectrophotometer. Fluorescence emission and fluorescence decay time measurements for the solutions and membranes were recorded using a fluorescence spectrometer and a picosecond

laser system described elsewhere [32]. PDMS membrane samples with 1 cm × 4 cm dimensions were placed onto quartz plates cut from a cuvette. The quartz plate was placed into the sample holder with an angle to minimize scattering further. Successive measurements with time showed no change in the spectra. Furthermore, repeated sample preparations, as described above, of the same zeolite sample also showed no change in the spectra. This has shown us that the precautions taken to exclude water of hydration were successful.

## 3. Results and discussion

### *3.1. Properties of zeolite Y samples*

The properties of the zeolite Y samples used in this study are given in table 1. The crystallinity of the sample HY-96 was low due to the uncontrolled removal of a large portion of the framework aluminum at the calcination stage. In the case of the USY sample the removal of the framework aluminum was carried out in steam which is thought to repair vacant sites by replacing the leaving aluminum with silica. The crystallinity of the samples was calculated by measuring the benzene adsorption isotherm and calculating the capacity at full loading. Although we have found the X-ray method to give a reasonable account of crystallinity, the diffraction line intensities are normally a function of other factors than crystallinity. For this reason the benzene adsorption capacity is used to measure the crystallinity, as it is a quantitative measure of the micropore volume, which in turn is a direct function of the zeolites structure.

The unit cell parameter $a_0$ decreases with the degree of exchange because increasing amounts of aluminum were removed from the framework as confirmed by $^{29}$Si and $^{27}$Al MAS NMR (shown in figure 1). The relationship between the unit cell parameter and the framework aluminum is found to be linear, figure 2, as proposed before [33]. From this relationship the framework aluminum in the USY sample was estimated as direct measurement by $^{29}$Si MAS NMR was not possible due to low sensitivity at this low concentration. It is estimated that the USY zeolite has 10 framework-aluminum sites per unit cell. The relationship may not be as linear as Breck and Flanigen originally proposed [33], but the correlation can be used semi-quantitatively. For USY zeolites used in fluid catalytic cracking the unit cell parameter is normally taken as an indication of the level of framework aluminum. MAS NMR of $^{27}$Al has shown that all the samples with the exception of the parent NaY have non-framework octahedrally coordinated aluminum. The proportion of octahedral aluminum relative to the framework aluminum increases with increasing percentage of H-form. Most of the non-framework aluminum exists as aluminum oxide and/or oxide hydrates. The $^{27}$Al MAS NMR of the USY sample consisted of a broad featureless peak covering the region −50–150 ppm relative to aluminum sulfate. This indicates that in USY, the non-framework aluminum is substantially polymeric and should be chemically inactive most probably due to the high temperature of steaming used in its preparation (815 °C).

Table 1

| Sample | UC $a_0$ (Å) | Number of Al (UC)[a] | Si/Al[a] | Pore capacity (wt%) | Benzene relative |
|---|---|---|---|---|---|
| NaY | 24.686 | 54.4 | 2.5 | 23.2 | 1.00 |
| HY-34 | 24.628 | 52.7 | 2.6 | 21.4 | 0.92 |
| HY-60 | 24.600 | 49.8 | 2.9 | 21.7 | 0.94 |
| HY-73 | 24.597 | 48.5 | 3.0 | 21.2 | 0.91 |
| HY-83 | 24.590 | 48.6 | 3.0 | 20.8 | 0.90 |
| HY-96 | 24.410 | 29.8 | 5.4 | 11.1 | 0.48 |
| USY-5c | 24.213 | 10[b] | 18[b] | 21.6 | 0.93 |

[a] Calculated from NMR spectra.
[b] Estimated from figure 2.

### *3.2. Fluorescence and excitation spectra*

The excitation spectra of NA, $\lambda_{em.} = 390$ nm, adsorbed on the surfaces of NaY catalyst, figure 3(a), shows that NA is present in the neutral form, $\lambda_{abs.,\,max} = 330$ nm. However, excitation spectra of NA adsorbed on the surfaces of protonated zeolite Y (HY-96) recorded at $\lambda_{em.}$ 340 nm, figure 3(a), shows that NA is present in the protonated form, $\lambda_{abs.} = 290$ nm. This means that a proton is transferred from the zeolite framework to the amino group of the NA in the ground state. The maximum is found at around 290 nm which corresponds to the absorption of a mixture of the protonated form $RNH_3^+$ and X of NA, where X is the newly found species described previously [32] and discussed below.

The fluorescence spectrum of NA adsorbed at the surface of zeolite NaY, figure 3(b), shows that NA is present in the neutral form ($RNH_2^*$). On the other hand, the fluorescence emission spectrum of NA adsorbed on the surface of HY-96, figure 3(b), shows that NA is present in both forms (the neutral $RNH_2^*$ and the protonated form $RNH_3^{+*}$). Furthermore, the absorption spectra of NA adsorbed on the surface of USY, figure 4(a), shows absorption corresponding to two species. The one recorded at $\lambda_{em} = 325$ nm corresponds to that of the protonated form while the one recorded at $\lambda_{em} = 400$ nm corresponds to another species. Fluorescence spectra of NA adsorbed on USY catalyst, $\lambda_{ex} = 276$ nm, figure 4(b) show only emission from the protonated form. Changing the excitation wavelength leads to a red shift in the emission wavelength and to a decrease in the fluorescence intensity. At $\lambda_{ex.} = 320$ nm the emission band is centered at 370–380 nm. This emission band corresponds to the species X* absorbing at 290 nm.

In a previous paper [32] we have studied the kinetics of NA in highly acidic medium using perchloric acid. It was found that at high acid concentration, where there are no free water molecules in solution, a new emitting species, we called it X, is formed. We reasoned that its formation is due to the lack of water molecules such that an adduct between the protonated NA ($RNH_3^+$) and the unhydrated perchlorate anion is formed leading to a complex X. This species was proposed on the evidence of the absorption and fluorescence spectra. It appeared to have a structure in between the base

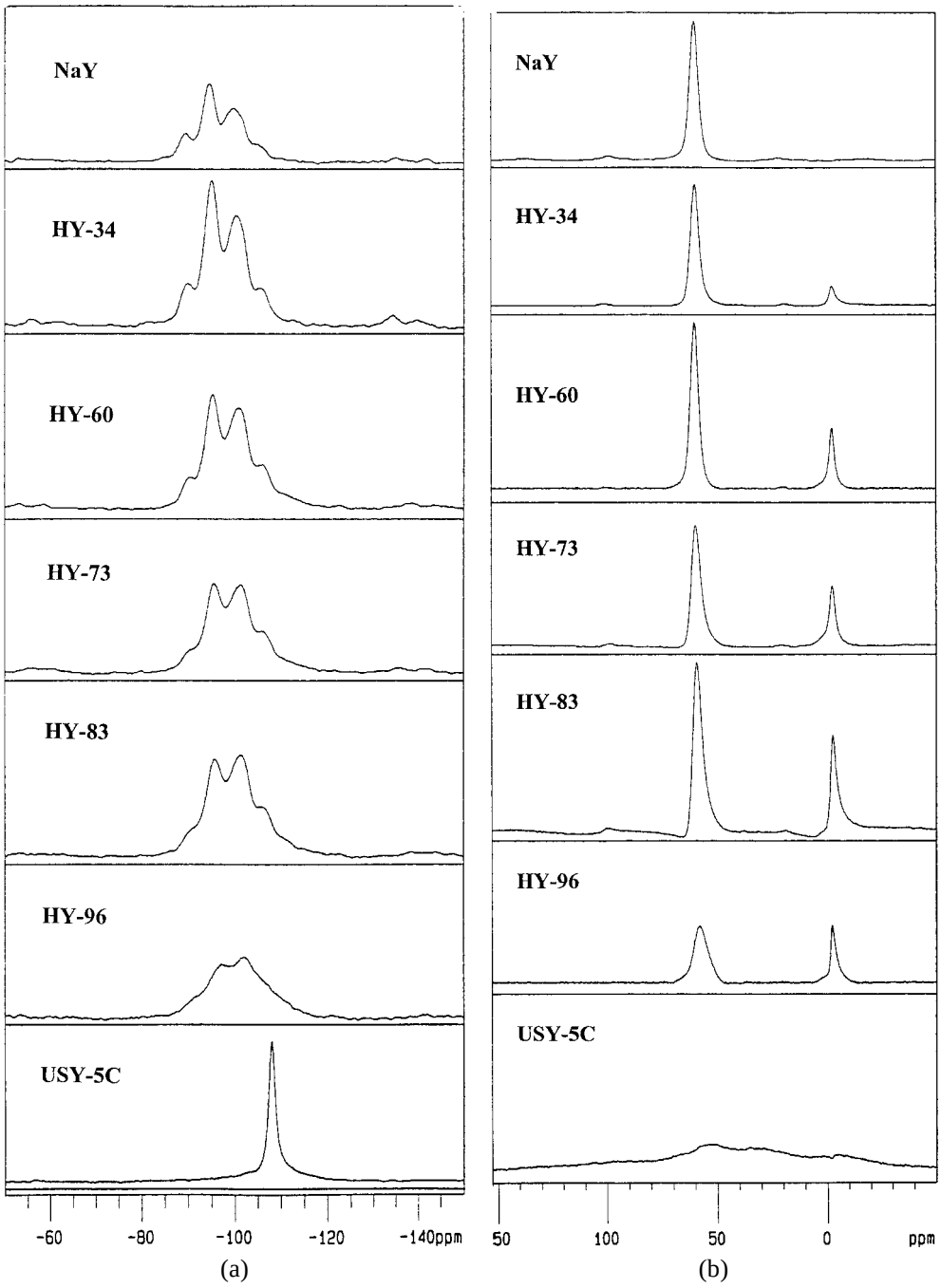


Figure 1. $^{29}$Si (a) and $^{27}$Al (b) MAS-NMR spectra of zeolite Y samples.

$RNH_2$ and its acidic form $RNH_3^+$. The proposal is consistent with the lack of free water for the hydration of the perchlorate anions and their lack of mobility.

The species X is the same one detected on the surface of zeolite Y. In the pores of the zeolite, there is no water of hydration and the mobility is restricted. Therefore a similar adduct formation with the anionic framework, "$RNH_3^+ \cdots Z^-$" is proposed. Both the absorption and fluorescence spectra of the zeolite Y series of samples show that the proportion of X increases with increasing acidity, *i.e.*, from HY-30 to USY. This trend is confirmed by our measurement of the fluorescence lifetime discussed below and can be explained on the basis of the non-framework aluminum species as follows.

In the case of low framework Si/Al ratio (samples HY-34 to HY-96), the presence of 1-NNN and 2-NNN aluminum, as shown by $^{29}$Si MAS NMR, figure 1, lowers the average acid strength of the surface. This results in a proton transfer reaction from the excited state of the protonated NA ($RNH_3^{+*}$, $pK_a = -1$) back to the zeolite surface. The fluorescence spectra of the NA in the zeolite samples show either the neutral form or a mixture with the protonated form. The low concentration of species X in these samples, relative to the USY, can be attributed to the presence of active octahedrally

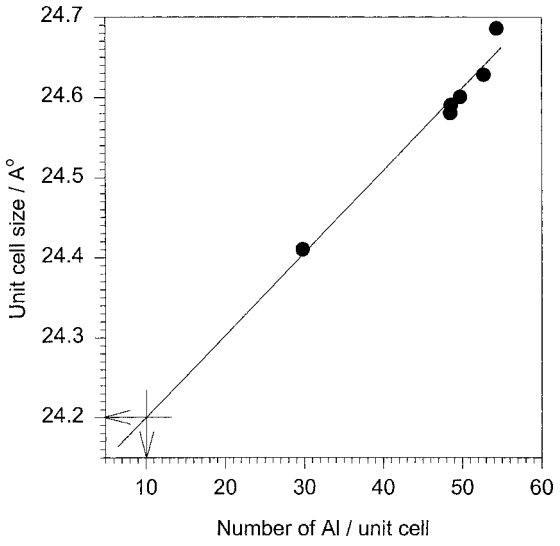


Figure 2. Unit cell parameter *vs.* the number of framework aluminum per unit cell.

coordinated aluminum oxide and oxide hydrate, as indicated by the $^{27}$Al MAS NMR, figure 1. These species can act as Lewis acids and stabilize the conjugate base of the Brønsted acid. Thus the protonated NA has a weak interaction with the framework anion and its fluorescence spectra are characteristic of the protonated NA. In the case of the USY, however, the non-framework aluminum species are shown by $^{27}$Al MAS NMR to be asymmetric and polymeric, most probably due to the high temperature of steaming (815 °C) used in the preparation of the sample. These aluminum species are chemically inert and not expected to stabilize the conjugate base. Although the acid site is of a high strength (0-NNN), the protonated NA must interact with the anionic framework leading to the formation of the "$RNH_3^+ \cdots Z^-$" species. Such interaction is promoted in the dry confines of the pore structure. Moreover, the amount of non-framework aluminum increases from the sample HY-34 to the USY further reducing the mobility of the species in the zeolite channels.

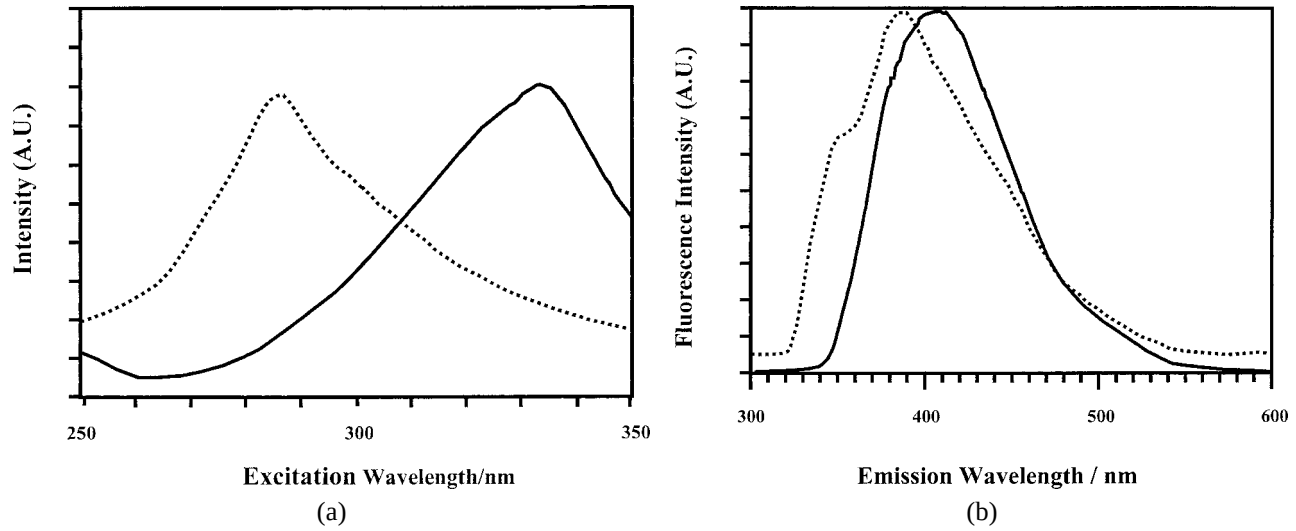


Figure 3. Excitation (a) and emission spectra (b) of NA adsorbed on NaY surfaces (—) and HY-96 surfaces (· · ·).

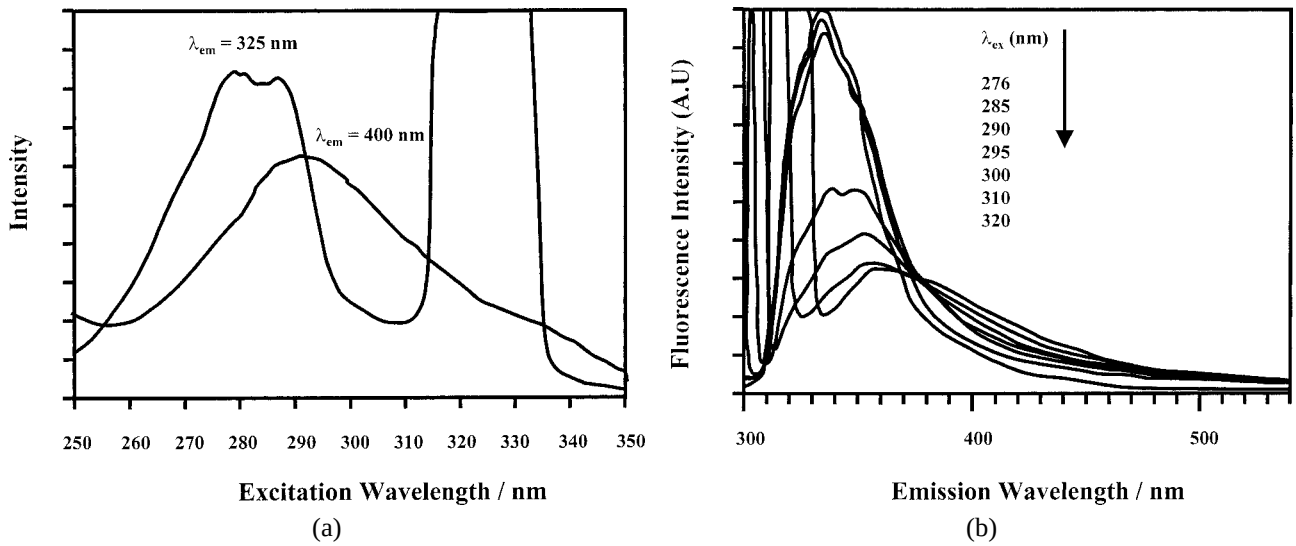


Figure 4. Excitation (a) and emission (b) of NA adsorbed on USY surfaces.

The excited state of the protonated form of NA is highly acidic and would only donate the proton back to the framework if the acid site is relatively less strong such as the case of the 2-NNN or even 1-NNN sites. In such a case the neutral form of NA is observed in the fluorescence spectra. The protonated form of NA is observed when large proportions of 0-NNN are present and only when there is active octahedrally coordinated aluminum oxide and oxide hydrate present in close proximity of the acid site. Otherwise X is formed as discussed above.

So at this point we can assign the absorption bands in figure 4(a) to both the protonated ($\lambda_{abs} = 276$ nm) and to the adduct X ($\lambda_{abs} = 290$ nm) forms of NA, respectively. Therefore, the emission spectra show predominant emission from the protonated form of NA as we excite at $\lambda_{abs} = 276$ nm, and upon increasing the excitation wavelength we excite more of the X form and so the emission maxima is shifted, figure 4(b).

In order to form an opinion about the chemical nature of the active centers at the catalyst surfaces we compared the absorption and fluorescence spectra of NA on zeolite Y of different percent protonation and at the USY catalyst. At low percent protonation (*e.g.*, HY-34), the absorption spectra show the absorption of both the protonated and the neutral form. However, by increasing the percent protonation, the spectrum is blue shifted and becomes quite similar to that of naphthalene which corresponds to the formation of $RNH_3^+$. This is obvious in the case of HY-96 catalyst and the USY catalysts.

The fluorescence spectra at the partially protonated forms of the zeolite, figure 3, show that the emission is mainly coming from the neutral form ($\lambda_{em}(RNH_2^*)$ is ~390 nm) with a little emission coming from the protonated form ($\lambda_{em}(RNH_3^{+*})$ is ~340 nm). The protonated form emission increases in intensity with increasing percent of protonation and at low loading level. The presence of only absorption of $RNH_3^+$ and fluorescence emission of both $RNH_3^{+*}$ and $RNH_2^*$ indicate that there is a proton transfer reaction in the excited state. Furthermore, the fluorescence bands are broad and structureless. The broad bands indicate complicated complex formation between the NA and the zeolite framework sites, these complexes are adsorbed at sites with different strength and what we see is the average, *i.e.*, is a superposition of isolated complexes of various strengths. However, in the USY catalyst, both absorption and emission are coming from the protonated NA and the X form, as shown in figure 4. This means that there is no proton transfer reaction in the excited state occurring on the surfaces, *i.e.*, the acid sites in USY are more acidic than the excited $RNH_3^{+*}$.

### 3.3. Fluorescence quantum yield and lifetime analysis

Quantum yields cannot be calculated directly from the emission spectra since the intensities of these spectra are highly affected by the geometry of the sample and the scattered light from the surface of the polymer films. However, lifetime measurements are more consistent and reflect the real surface interactions with the probe molecule.

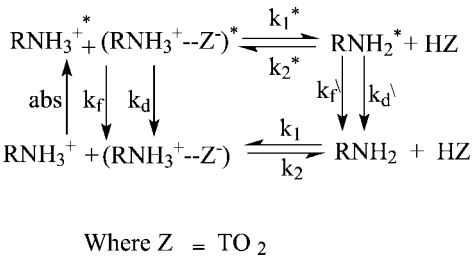


Scheme 1. Proton transfer reactions of $RNH_2$ (naphthylamine) with the Brønsted acid sites of the zeolite surface in the ground and the first singlet excited state.

In the zeolite framework, Si and Al atoms are tetrahedrally bonded through oxygen linkage to form the cages and channels. This gives rise to the formation of both $TO_2$ "a weak Lewis base site" if the tetrahedral atoms (T) and their neighbors are all Si and $HTO_2$ "a Brønsted acid site" if the tetrahedral atoms (T) or one of its neighbors is Al. Adsorption of $RNH_2$ on a Brønsted acid site leads to the formation of either the $RNH_3^+$ or $X \equiv RNH_3^+ \cdots TO_2^-$, depending upon the strength of the acid site.

The proton transfer reaction scheme of $RNH_2$ adsorbed at the zeolite surfaces is represented in scheme 1.

Fluorescence decay analysis recorded at $\lambda_{em.} = 330$ nm shows that the decay is bi-exponential with the short living component assigned to $RNH_3^+ \cdots Z^{-*}$ and a long living one corresponding to $RNH_3^{+*}$, table 3. The decay of the short living component is clearly seen to be more likely formed at high percent protonated zeolite, *i.e.*, highly acidic environment. The change in the decay profile upon protonation of the zeolite Y is shown in figure 5. The fluorescence decay rate constant "$\lambda = k_f + k_q$" for $RNH_2^*$ in the zeolite cages is found to vary from $1.54 \times 10^8$ to $1.17 \times 10^8$ $s^{-1}$ depending upon the protonation level of the catalyst, which is fairly fast compared to the value of $5.5 \times 10^7$ $s^{-1}$ for free $RNH_2^*$ in solution. This means that the zeolite framework destabilizes the excited state of neutral 1-naphthylamine in comparison to aqueous solutions. The deactivation mechanism for excited 1-naphthylamine may be accounted for by the high basicity of the excited state of $RNH_2$ that makes it more susceptible to be attacked by the various Lewis and Brønsted acid sites from the zeolite framework, *i.e.*, $RNH_2^*$ is strongly quenched by the surrounding environment, $k_f$ and $k_q$ cannot be separated as quantum yield measurements are not feasible as mentioned before.

Formation of both $RNH_3^+$ and X at the surfaces of zeolite Y can be accounted for by the fact that the zeolite surfaces contain sites with different acidic strength. According to our $^{29}Si$ and $^{27}Al$ NMR results, we have 2-NNN, 1-NNN and 0-NNN acid sites with the Brønsted acid strength increasing in this order. In all cases adsorption of NA at the surfaces of the catalyst leads to protonation in the ground state. However, upon excitation $RNH_3^{+*}$ becomes a very strong acid ($pK_a = -1$) and tends to dissociate and protonate the surface site. In this case, if the surface site is a

Table 2
Absorption and fluorescence. $\lambda_{max}$ (nm) and fluorescence lifetimes[a] of X* and $RNH_3^{+*}$ in different protonated forms of zeolite Y and the estimated acidities

| Catalyst | Loading level[b] | Absorption $\lambda_{max}$ (nm) | Fluorescence $\lambda_{max}$ (nm) | $\tau_1$ (ns) | $A_1$ | $\tau_2$ (ns) | $A_2$ | $[H^+]^c$ |
|---|---|---|---|---|---|---|---|---|
| HY-34 | 0.05 | 290 | 330, 390 | 1.46 | 0.575 | 7.58 | 0.514 | 3.69 |
| HY-60 | 0.05 | 280 | 340, 390 | 1.62 | 0.581 | 8.66 | 0.501 | 5.70 |
| HY-73 | 0.04 | 275 | 330, 410 | 1.78 | 0.389 | 8.24 | 0.208 | 7.81 |
| HY-83 | 0.05 | 280 | 330, 400 | 1.91 | 1.37 | 8.21 | 0.261 | 9.47 |
| HY-96 | 0.04 | 280 | 330, 390 | 2.24 | 2.76 | 9.76 | 0.313 | 13.7 |
| USY-5c | 0.04 | 276, 290 | 330, 370 | 2.50 | 0.607 | 18.8 | 0.612 | 17.0 |

[a] $\lambda_{exc.} = 300$ nm, $\lambda_{em.} = 340$ nm.
[b] Loading level expressed as molecule/unit cell.
[c] Estimated using the fitting equation of figure 6.

Table 3
Absorption and fluorescence $\lambda_{max}$ and decay time[a] constants for the acidic form of 1-naphthylamine (NA) in different protonated forms of zeolite Y

| Catalyst | Loading level[b] | Absorption $\lambda_{max}$ (nm) | Fluorescence $\lambda_{max}$ (nm) | $\tau_1$ (ns) | $A_1$ | $\tau_2$ (ns) | $A_2$ | $[H^+]^c$ |
|---|---|---|---|---|---|---|---|---|
| HY-34 | 7.6 | 330 | 420 | 1.38 | 1.54 | 5.26 | 0.884 | 2.66 |
| | 4.03 | 290, 330 | 340. 390 | 1.40 | 1.35 | 6.18 | 0.783 | 2.90 |
| | 0.45 | 290 | 340, 390 | 1.41 | 1.64 | 7.11 | 0.552 | 3.05 |
| HY-60 | 7.3 | 290, 330 | 420 | 1.50 | 0.965 | 5.83 | 1.40 | 4.20 |
| | 3.87 | 290, 330 | 420 | 1.53 | 0.696 | 6.17 | 1.05 | 4.59 |
| | 0.44 | 280 | 340, 390 | 1.56 | 1.22 | 7.90 | 0.672 | 4.90 |
| HY-73 | 7.2 | 285, 330 | 340, 410 | 1.65 | 0.701 | 7.15 | 0.880 | 6.20 |
| | 3.8 | 285, 330 | 340, 390 | 1.68 | 1.25 | 7.86 | 0.668 | 6.57 |
| | 0.43 | 290 | 330, 410 | 1.76 | 1.12 | 8.06 | 0.531 | 7.54 |
| HY-83 | 6.9 | 290, 330 | 330, 400 | 1.81 | 0.508 | 6.20 | 0.649 | 8.19 |
| | 3.8 | 290 | 330, 390 | 1.83 | 0.823 | 6.56 | 0.666 | 8.45 |
| | 0.429 | 285 | 330, 420 | 1.85 | 1.11 | 7.14 | 0.337 | 8.70 |
| HY-96 | 6.30 | 290 | 335, 420 | 2.01 | 0.434 | 7.32 | 0.427 | 10.8 |
| | 3.06 | 290 | 330, 410 | 2.12 | 0.493 | 8.94 | 0.369 | 12.2 |
| | 0.306 | 285 | 330, 390 | 2.17 | 0.447 | 9.49 | 0.486 | 12.8 |
| USY | 6.30 | 280, 310 | 340, 400 | 1.99 | 0.945 | 13.7 | 1.13 | |
| | 3.06 | 276, 290 | 340, 400 | 2.11 | 0.850 | 16.9 | 1.23 | |
| | 0.306 | 276, 290 | 340, 370 | 2.31 | 0.607 | 17.8 | 0.612 | |

[a] $\lambda_{exc.} = 300$ nm, $\lambda_{em.} = 340$ nm.
[b] Loading level expressed as molecule/unit cell.
[c] Estimated using the fitting equation of figure 6.

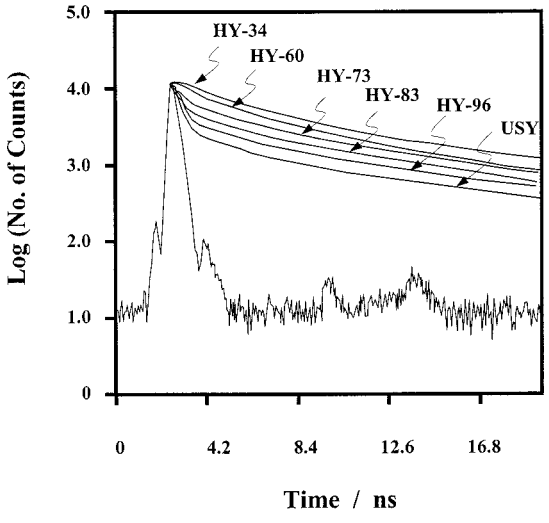


Figure 5. Emission decay of NA/HY, different protonation level and unit cell size.

weaker acid site it would be protonated and we get fluorescence corresponding to the neutral form $RNH_2^*$. If the surface site is strongly acidic, it will not accept the proton, and in such a case both $RNH_3^{+*}$ and the X* form are formed depending on the state of the non-framework aluminum present as discussed above. In this case fluorescence due to the two forms is expected and so the fluorescence decay time is fitted with a bi-exponential function.

From our study of the excited state reaction of NA in aqueous acidic solution [32], we found that the lifetime of $RNH_3^{+*}$ increases with the acidity of the medium in the presence of free water molecules till it reaches a maximum and then decreases in the absence of free water. This decrease is accompanied by the formation of X.

The maximum lifetime for $RNH_3^{+*}$ in the catalyst (USY) is found to be 18.8 ns indicating that the quantum yield of $RNH_3^{+*}$ is about 2.4 times less than the maximum quantum yield ($\Phi = 0.327$) in aqueous solution of $HClO_4$.

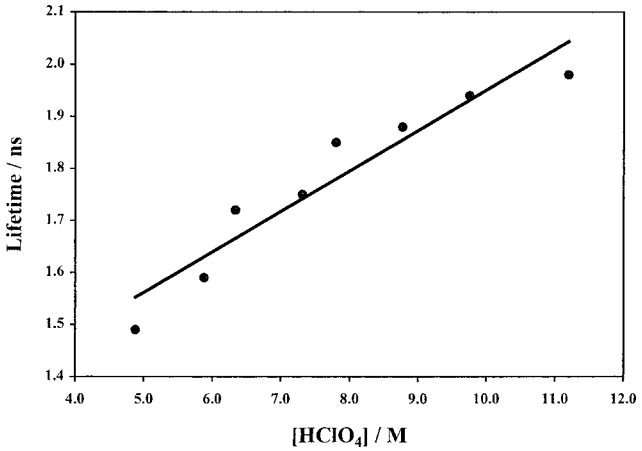


Figure 6. Fluorescence decay time $\tau$ of X ($RNH_3^{+*}\cdots Z^-$) as a function of molarity of perchloric acid.

Also from our study of the excited state reactions of NA in acidic solution, we found that the formation and the lifetime of X* is a function of the acidity of the medium, figure 6. The straight-line equation for that relation is $\tau = 0.078[H^+] + 1.17$, with an $R^2$ value of 0.91 [32]. From this relation, by inserting the value for $\tau$ found in the zeolite, we are able to estimate the relative acidity inside the zeolite cages. The estimated acidity is given in table 2. These values reflects the highly acidic environment experienced by NA inside the cage. It is clearly seen that the estimated acidity increases with reduction in the unit cell size. A plot of the estimated acidity *vs.* the corresponding lifetime using the equation

$$\frac{\tau_{max.}}{\tau} = 1 + \frac{k_d}{k_f}[H^+]$$

gives a linear Stern–Volmer relation, figure 7. From the slope of the fitted line, $k_d$ is calculated to be $2.1 \times 10^7$ s$^{-1}$, which is much less than the value found for X* in solutions ($4.7 \times 10^8$ s$^{-1}$). This means that the zeolite framework stabilizes and enhances the formation of X*. The enhancement of X is also due to the absence of free water molecules. We

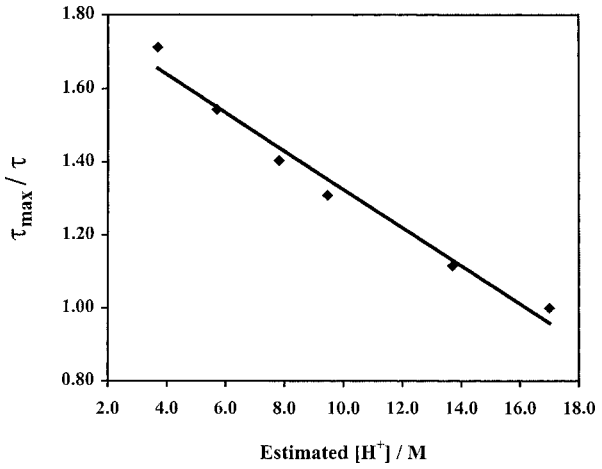


Figure 7. Relative fluorescence decay time $\tau_{max.}/\tau$ of ($RNH_3^{+*}\cdots Z^-$) as a function of the estimated acidity of the zeolite.

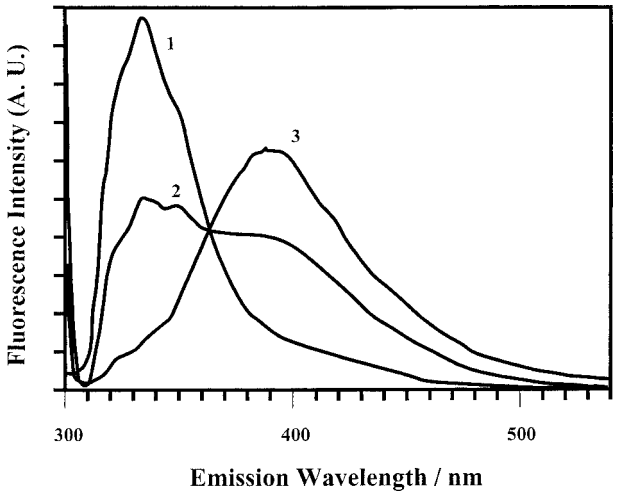


Figure 8. Fluorescence emission spectra of NA adsorbed on USY surfaces at different loading levels, 0.05 (1), 3.87 (2), and 7.3 molecules/unit cell (3).

have not been able to find a Stern–Volmer plot for proton-transfer reaction at zeolite Y surfaces in order to compare our findings with it.

Concentration effects are taken into account by varying the loading level of the adsorbed molecule. It is found that at high loading level the excitation spectra correspond to mainly the absorption of the neutral form only. Furthermore, the fluorescence spectra at high loading level also show mainly the emission from the neutral form of the amine. This can be accounted for by other interactions than protonation at the active centers. In this case one may assume that due to the bulkiness of the NA molecules and the small space available for additional molecules to move in, they could be positioned in the cage in an opposite direction to the Brønsted acid sites. Therefore, the interaction between the amino groups of additional molecules and the active sites is suppressed. Furthermore, some of the NA molecules could be located outside the pores leading to no possibility for interacting with acidic sites. By lowering the loading levels, the spectrum is blue shifted indicating more interactions with acidic sites, figure 8. The interactions between acidic sites inside the cage and the probe molecules at low loading levels is similar to that experienced by the probe molecule in highly acidic solutions. Estimated acidities for the catalysts at the various loading levels are given in table 2. However, in case of low loading we expect the probe molecule to be surrounded by a variety of Brønsted acid sites of different strengths. Figure 9 shows the decay profile of NA adsorbed at HY-60 at different loading levels. It is obvious that the short decaying component is dominant at low loading level, where more acid sites are accessible for the NA.

The acid strength may also be correlated to the unit cell size. Figure 10 shows that the average acid strength increases with reduction in the unit cell size. This correlation can only be accounted for by the increase in the percentage of 0-NNN sites and its superior acid strength. The current study is, therefore, in accord with the NNN theory of acidity in zeolite Y and seems to explain the role of the non-

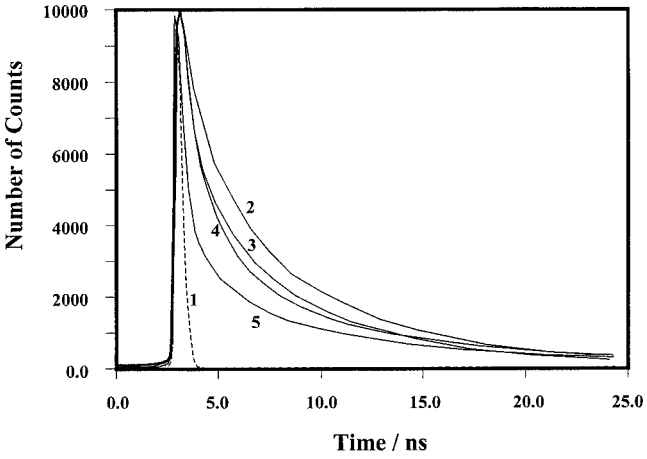


Figure 9. Emission decay of NA/HY-60 at different loading levels, pump pulse (1), 7.3 (2), 3.87 (3), 0.44 (4), and 0.05 (5) molecules/unit cell (3).

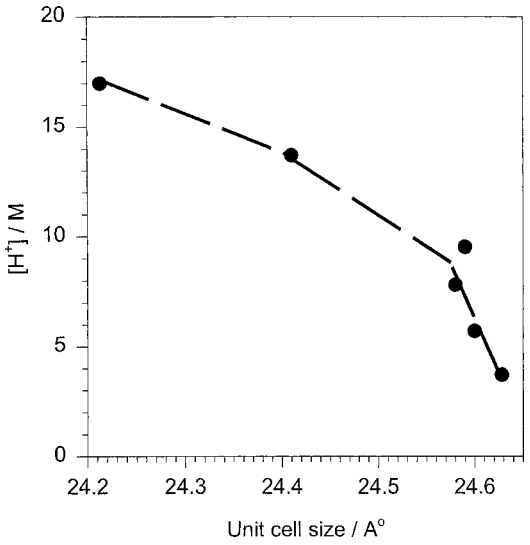


Figure 10. Correlation between the estimated average acid strength and the unit cell size.

framework aluminum as being only important when it is in an active form and able to interact with the conjugate base of the Brønsted acid site. The degree of the acid site isolation is the primary factor influencing its strength.

## 4. Conclusions

Proton transfer reactions between zeolite Y surface and 1-naphthylamine (NA) in the ground and excited states have been studied by laser-induced picosecond spectroscopy. The acid form of the zeolite readily protonates NA in the ground state. At low acid strength, the excited state of the protonated amine form donates the proton back to the zeolite surface as indicated by the fluorescence spectra. At high acid strength, the fluorescence comes from the protonated NA, when there is active non-framework aluminum to interact with the anionic surface. When the non-framework aluminum becomes polymeric, the protonated amine interact with the conjugate base on the zeolite surface and forms the adduct X ($RNH_3^+ \cdots Z^-$). The species X is found in the ground and excited states. The relative concentrations of protonated NA and X increase with reduction in the unit cell size. The presence of these species and their relative concentrations have been discussed in terms of the next nearest neighbor "NNN" theory of zeolite Y acidity and the role of the non-framework aluminum.

The lifetimes of X in solutions is used to estimate the acidity inside the zeolite cages. It is found to be equivalent to 3.7 M $HClO_4$ acid for HY-34, 5.7 M acid for HY-60, 7.8 M acid for HY-73, 9.5 M acid for HY-83, 13.7 M acid for HY-96 and 17.0 M for the USY catalyst. Low loading levels of the amine are found to give better results than higher loading levels, where other interactions than protonation at the amino group are expected.

## Acknowledgment

Support from King Fahd University of Petroleum and Minerals is gratefully acknowledged. The authors also appreciate the opportunity given by Dr. M.A. Garwan and Dr. H. Al-Masoudi from the Center for Applied Physical Sciences (CAPS), Research Institute to use the laser facility.

## References

[1] R.A. van Santen and G.J. Kramer, Chem. Rev. 95 (1995) 637.
[2] A. Corma, Chem. Rev. 97 (1997) 2373.
[3] E.W. Hansen, F. Courivaud, A. Carlson, S. Kolboe and M. Stocker, Micropor. Mesopor. Mater. 22 (1997) 309.
[4] S. Biz and M.L. Occelli, Catal. Rev. Sci. Eng. 40 (1998) 329.
[5] Mirodatus and D. Bathomeuf, J. Catal. 93 (1985) 246.
[6] A. Corma, H. Garcia, S. Iborra and J. Primo, J. Catal. 120 (1989) 78.
[7] C.V. McDaniel and P.J. Maher, in: *Conference on Molecular Sieves* (Society of Chemical Industry, London, 1967) p. 186.
[8] G.T. Kerr, in: *Molecular Sieves*, Adv. Chem. Ser., Vol. 121, eds. W.M. Meier and J.B. Uytterhoeven (1973) p. 219.
[9] P.A. Jalil, M.A. Al-Daous, A.A. Al-Arfaj, A.M. Al-Amer, J. Beltramini and S.A.I. Barri, Appl. Catal. A 207 (2001) 159.
[10] G.T. Kerr, J. Phys. Chem. 73 (1969) 2780.
[11] G.W. Skeels and E.M. Flanigen, in: *Zeolite Synthesis*, Adv. Chem. Ser., Vol. 435 (1989) p. 420.
[12] L.A. Pine, P.J. Maher and W.A. Wachter, J. Catal. 85 (1984) 466.
[13] A.A. Eremenko, F.M. Bobonitz, M.V. Cost, M.A. Pionkovskaya, M.Yu. Sakhnovskii and I.E. Niemark, Opt. Spektrosk. 35 (1973) 224.
[14] B.H. Bartez and N.J. Turro, J. Photochem. 24 (1984) 201.
[15] P. Hite, R. Krasnansky and J.K. Thomas, J. Phys. Chem. 90 (1986) 5295.
[16] J.K. Thomas, J. Phys. Chem. 91 (1987) 267.
[17] J.K. Thomas, Chem. Rev. 93 (1993) 301.
[18] X. Liu, K.K. Iu and J.K. Thomas, J. Phys. Chem. 93 (1989) 4120.
[19] X. Liu, K.K. Iu and J.K. Thomas, J. Phys. Chem. 98 (1994) 7877.
[20] B.H. Milosavljevic and J.K. Thomas, J. Phys. Chem. 92 (1988) 2997.
[21] H. Shizuka, Acc. Chem. Res. 18 (1985) 141.
[22] A. Corma, M.S. Grande, V. Gonzales Alfaro and A.V. Orchilles, J. Catal. 159 (1996) 375.
[23] S.A. Rutten and J.K. Thomas, J. Phys. Chem. B 102 (1998) 598.
[24] N.J. Turro, Pure Appl. Chem. 58 (1986) 1219.
[25] V. Ramamurthy, J. Am. Chem. Soc. 116 (1994) 1345.

[26] J.C. Scaiano, N.C. De Locas, J. Andraos and H. Garcia, Chem. Phys. Lett. 233 (1995) 5.
[27] S. Corrent, P. Hahn, G. Pohlers, T.G. Connoly, G.C. Scaiano and H. Garcia, J. Phys. Chem. B 102 (1998) 5852.
[28] M. Alvaro, H. Garcia, S. Corrent and J.C. Scaiano, J. Phys. Chem. B 102 (1998) 7530.
[29] I.F.J. Vankelecom, D. Depre, S.D. Beukelaeur and J.B. Uytterhoeven, J. Phys. Chem. B 99 (1995) 13193.
[30] I.F.J. Vankelecom, C. Dotremont, M. Morbe and J.B. Uytterhoeven, J. Phys. Chem. B 101 (1997) 2154.
[31] C. Dotremont, I.F.J. Vankelecom, M. Morbe and J.B. Uytterhoeven, J. Phys. Chem. B 101 (1997) 2160.
[32] A.A. El-Rayyes, H.P. Perzanowski, S.A.I. Barri and U.K.A. Klein, J. Phys. Chem., accepted.
[33] D.W. Breck and E.M. Flanigen, in: *Conference on Molecular Sieves* (Society of Chemical Industry, London, 1967) p. 47.